Differential cross sections for charged-particle emission in reactions of 58-MeV α particles with ^{12}C, ^{16}O, and ^{54}Fe: Comparison with the exciton model of pre-equilibrium particle emission*

F. E. Bertrand and R. W. Peelle
Oak Ridge National Laboratory, Oak Ridge, Tennessee 37830

C. Kalbach-Cline†‡
Nuclear Structure Research Laboratory § and Chemistry Department, University of Rochester, Rochester, New York 14627
(Received 9 May 1974)

Cross sections differential in energy and angle are presented for the proton, deuteron, triton, and α particles from reactions of 58-MeV α particles on C, O, and ^{54}Fe, and the angle-integrated differential spectra are compared with the predictions of an extended exciton model of pre-equilibrium reactions. The experimental results were obtained with a semiconductor telescope and cover the whole energy range above a few MeV. Except for oxygen, the results are given with uncertainties of 5–10%; for oxygen, relative intensities are valid at a given angle, but the absolute uncertainty is about 50%. The high-energy segment of the spectrum is highly anisotropic for all emitted particles, but for low energies the evaporation mechanism may be important for proton and perhaps α-particle emission. The inelastic α spectra from ^{54}Fe are more similar in shape to previous observations of the $^{54}Fe(p,xp)$ spectra than to the presently reported $^{12}C(\alpha,x\alpha)$ results. Comparisons are made between the data and the exciton model assuming an initial configuration of four particles. The model was extended to recognize that for reactions of incident α particles, emitted α particles and even deuteron, triton, and ^3He particles may contribute a significant fraction of the pre-equilibrium emission. The empirical internormalization factor for the relative intensity of various exit particles (mass number p_β) is found to be consistent with the (p_β !) value deduced previously from results with incident protons. Using matrix elements deduced from systematics, the predictions for ^{12}C yield qualitatively correct shapes with normalization for the various particle types correct to within a factor of 6. For ^{54}Fe, the magnitude and shape of the predicted integral spectra are good for secondary protons and deuterons, but the predicted spectra fall off far too rapidly at high energies for tritons and α particles.

[NUCLEAR REACTIONS ^{12}C, ^{16}O, ^{54}Fe, $(\alpha, \alpha' x)$, (α, tx), (α, dx), (α, px), $E = 58$ MeV; Ge(Li); measured $\sigma(E_{\alpha'}, E_t, E_d, E_p, \theta)$; deduced $\sigma(E)$. $2 \lesssim E_\alpha, E_t, E_d, E_p \lesssim 60$ MeV. Comparison with extended exciton model of preequilibrium particle emission.]

I. INTRODUCTION

To complement studies of reaction mechanisms which lead to population of particular nuclear states, it is important to obtain at least a semiquantitative understanding of the mechanism of the bulk of the reactions which occur when a target is bombarded with medium-energy projectiles. To enable such understanding, experimental measurements are required for several types of emitted particles over essentially their entire energy ranges. The applicable calculations tend, so far, to be statistical in their approach and depend relatively little on details of nuclear structure.

An important physical question is whether experimental results can be reproduced from the known general properties of nuclei, and practical applications often require the similar ability to estimate nuclear cross sections where measurements have not been performed. This paper examines whether the exciton model can explain emission of proton, deuteron, triton, and α particles in reactions induced by 58-MeV α particles on C, O, and ^{54}Fe. Previous empirical studies have not made such an analysis possible.

Although many studies of inelastic α-particle scattering or α-induced transfer reactions have been performed, these experiments have nearly always been insensitive to the emitted particles beyond the first few MeV of excitation energy. Thus, there exists little information on the spectral region which, for medium-energy reactions, includes the major portion of the particle emission. During a series of experiments[1] which investigated similar particle spectra from incident 30- to 60-MeV protons, some data were obtained using 58-MeV α particles on targets of C, O, and ^{54}Fe. Separated spectra of emitted protons, deuterons, tritons, and α particles were recorded over an energy range from ~2 MeV up to the full energy kinematically allowed.

The exciton preequilibrium statistical model,

initially proposed by Griffin[2] and subsequently extended and modified by several authors,[3-5] has been used to describe semiquantitatively the secondary proton and neutron spectra from targets bombarded by protons and α particles. Recently, a further extension of this model has been published[6] in which the spectra and relative intensities of secondary complex (deuteron, triton, α, etc.) particles emitted by targets bombarded by 30- to 60-MeV protons were calculated and compared to experimental results. It is possible to test the model's application for incident α particles using the data presented here where the experiment covers the competition among various emitted charged particles.

II. EXPERIMENTAL METHOD

The entire data collection and analysis system has been described in detail.[7] α particles of energy 58.8 MeV were obtained from the Oak Ridge isochronous cyclotron and momentum analyzed in a 153° magnet. The charged reaction products from the target were detected in a three-element semiconductor spectrometer telescope utilizing lithium-drifted germanium as the total absorption detector.[8] The germanium detector was isolated from the scattering chamber by a ~3-mg/cm^2 nickel foil. The thickness of this foil and that of the targets (~3 mg/cm^2), while not a significant contributor to the hydrogen-particle energy resolution of ~180 keV full width at half-maximum (FWHM), produced much of the considerable broadening (up to 1 MeV) observed for helium particles. An aperture in a 1-mm-thick plastic scintillator was used as the collimator for the counter telescope (see Ref. 7).

Secondary particle type was determined by a combination of $\Delta E \times E$ and time of flight vs. E methods in order to cover an energy range of ~2–60 MeV. A malfunction of the first silicon ΔE detector (~100 μm) during this particular experiment made very uncertain the separation below ≈33 MeV of ^{3}He from ^{4}He particles. Above 33 MeV for ^{3}He and ^{4}He, and for protons, deuterons, and tritons at all energies, identification of particle type was unambiguous. Since the cross section for ^{3}He production is substantially less than that for ^{4}He, the uncertainty in the separation had little effect on the ^{4}He data, but the cross sections for the ^{3}He production may be in doubt by as much as 50%. For this reason, only an integral over energy and angle is given for the ^{3}He emission.

The 97.2% enriched, 3.33-mg/cm^2 target of ^{54}Fe was fabricated by the Isotopes Division of the Oak Ridge National Laboratory. The carbon data were taken using a polystyrene (CH) foil, and the oxygen data were obtained from a foil of $C_{12}H_{16}O_8$ (Kodacel). Details of the properties of the three targets, along with an analysis of the systematic errors in the data, may be found in Ref. 9. The overall systematic uncertainty is 7–10% for the C and Fe cross sections. The α-p scattering peaks were manually removed from the C and O data.

In order to extract the ^{16}O data from the composite spectra obtained from the Kodacel foil, carbon data taken at the same angle in an adjacent run were subtracted from the composite. The subtraction of ^{12}C was carried out by normalization at each scattering angle of the measured ^{12}C spectrum for the elastic scattering, 4.43-MeV ^{12}C level or the ^{12}C(p, d) ground state to that observed in the composite (O+C) spectra from the Kodacel foil. Since one or more of these peaks were always clearly visible in the composite spectra, the effective carbon surface density for the Kodacel foil was adjusted until the ^{12}C peaks were no longer visible in the net (oxygen) spectra. The Kodacel gradually deteriorated under bombardment, so the absolute normalization for the ^{16}O data is uncertain, and the errors in the absolute cross sections are given as ±50%. The relative particle intensities at a given angle are unaffected, but angle-integrated spectra were too unsure for comparison with calculations.

TABLE I. Integral laboratory system emission cross sections and average energies for incident 58-MeV α particles.

Detected particle	Integral cross section[a] (mb)	Average emitted energy (MeV)	Low-energy cutoff (MeV)
	^{12}C		
Proton	395 ± 48	10.8	2.0
Deuteron	168 ± 22	12.3	2.0
Triton	33 ± 4	17.1	5.9
^{3}He	37 ± 19	23.3	13.6
α	1117 ± 136[b]	15.5[b]	4.8
	^{16}O		
Proton	420 ± 210	10.3	2.4
Deuteron	128 ± 64	14.1	2.5
Triton	22 ± 11	18.5	6.0
^{3}He	21 ± 10	25.5	13.8
α	755 ± 372[b]	15.2[b]	5.0
	^{54}Fe		
Proton	2274 ± 160	7.9	1.9
Deuteron	126 ± 9	17.3	2.2
Triton	25 ± 2	26.7	5.8
^{3}He	33 ± 16	31.3	13.4
α	642 ± 45[b]	17.9[b]	5.7

[a] Uncertainties are absolute and reflect all sources of error.

[b] Excludes elastic scattering.

The data shown in the figures have been corrected to remove in first order the effects of energy loss in the target and in the nickel window over the germanium detector. The effect of nuclear reactions of the hydrogen particles in the Ge detector was also compensated. The corrected particle spectra often show a local distortion at the energy corresponding to particles ending their range in the nickel foil which covered the germanium detector, but these distortions are seldom visible or significant in spectra averaged over energy regions as large as 1 MeV. For instance, in the spectra shown on Fig. 2 only the 20° proton and deuteron spectra show this spurious ($\lesssim$10%) effect. These discontinuities in the spectra appear at the scattered energies necessary to reach the Ni foil, approximately 9, 12, and 15 MeV for protons, deuterons, and tritons, respectively, and 35 MeV for α particles. The average cross section over a region within ±20% of these energies was not affected by this experimental effect or its correction.

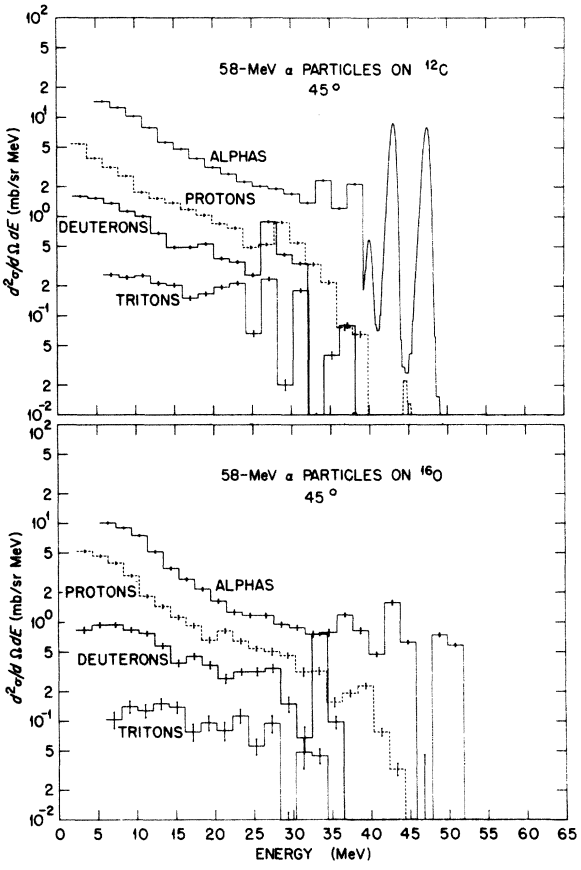

FIG. 1. Charged-particle spectra from ^{12}C and ^{16}O bombarded by 58-MeV α particles. θ_{lab}=45°. Except for the high-energy proton and α-particle spectra from ^{12}C, the data are shown averaged in 2-MeV wide bins for ease of comparison between particle types. The absolute cross section for the ^{16}O spectra are uncertain by ≈ 50% (see text). However, the relative intensities of the various secondary particles from ^{16}O are accurate to ≈ 10%.

The low-energy cutoff for each spectrum was determined by the target thickness or by ambiguities introduced by recoil heavy particles ($A>4$) in the time-of-flight identification system. Only a small fraction of the cross section was omitted from the results because of the cutoff energies given in Table I.

III. EXPERIMENTAL RESULTS

Tabulated experimental cross sections (mb sr^{-1} MeV^{-1}) may be obtained from Ref. 9. This tabulation lists binned cross sections for each spectrum at each angle of observation, along with derived cross sections integrated over either angle or energy.

A. ^{12}C and ^{16}O

Figure 1 shows the binned 45° spectra of protons, deuterons, tritons, and α particles from ^{12}C and ^{16}O. The spectra are all plotted on the same scale to indicate the relative yields of the various particles. These and the corresponding spectra at other angles show that the proton-to-deuteron ratio is approximately the same for ^{12}C and ^{16}O. However, the α/p ratio is smaller for ^{16}O than ^{12}C.

The charged-particle spectra from ^{12}C are shown at several angles on Fig. 2. While the secondary α, deuteron, and proton spectra at small angles show a low-energy peak, at larger angles the kinematic shift in the laboratory emission energies places any low-energy cross section out of the detection range of our system. In all cases the high-energy portions of the spectra are dominated by inelastic scattering and stripping reactions leading to bound states of the residual nuclei. Unlike the inelastic continuum spectra observed from incident proton bombardment (see Fig. 2, Ref. 1) and unlike the inelastic α spectra from ^{54}Fe to be shown below (Fig. 4), the α spectra from ^{12}C all steadily increase in magnitude toward the lower energies until the spectra are found to "turn over" at an energy somewhat below the Coulomb barrier. (A direct graphic comparison is shown in Fig. 21 of Ref. 9.)

Figure 3 shows the emitted proton, deuteron, triton, and α-particle spectra for carbon integrated over angle in the lab system. Table I shows the integrated (over angle and energy) laboratory system cross section for the production of each particle type above the low-energy cutoff shown. The table also shows the measured average emitted energy for each particle type.

B. ^{54}Fe

The 30° proton, deuteron, triton, and α spectra from ^{54}Fe are shown in Fig. 4. The α-emission spectrum shows a rather flat continuum between the high-energy inelastic peaks and the prominent low-energy peak. A similar spectral shape was found for protons emitted from ^{54}Fe bombarded by 62-MeV protons (see Fig. 4, Ref. 1). Below the region of distinct structure, the secondary deuteron and triton spectra are similarly flat; however, no strong low-energy peak is observed. The proton spectra are dominated by the large low-energy cross section, but a significant high-energy "tail" extends to the maximum energy kinematically allowed. This (α, xp) spectrum has a shape similar to those obtained at 30, 42, and 54 MeV on similar mass targets.[10-12]

The charged-particle spectra from ^{54}Fe are shown in Fig. 5 at a few angles. Kinematic shifts in the low-energy peaks are observable. All the spectra show a strong angular dependence, particularly for the high-energy region.

The proton and α cross sections in the low-energy peak are smallest at 90°. This effect has been studied in detail at 20-MeV incident energy by Benveniste, Merkel, and Mitchell.[13] These authors found that the angular distributions of the low-energy peak from the (α, α') and (α, p) reactions were symmetric about 90°. Evaporation calculations which included conservation of angular momentum explained the observed cross sections.

The secondary α-particle spectra of Fig. 5 show at the smaller angles a cross-section enhancement in the continuum at ≈37 MeV. The error bars on two of the cross-section bins have been increased because this region is affected by the stopping of particles in the nickel window. However, an indication of cross-section enhancement may persist beyond these increased errors. There have been several recent papers discussing excitation of giant resonances by protons[14] and α particles[15] and

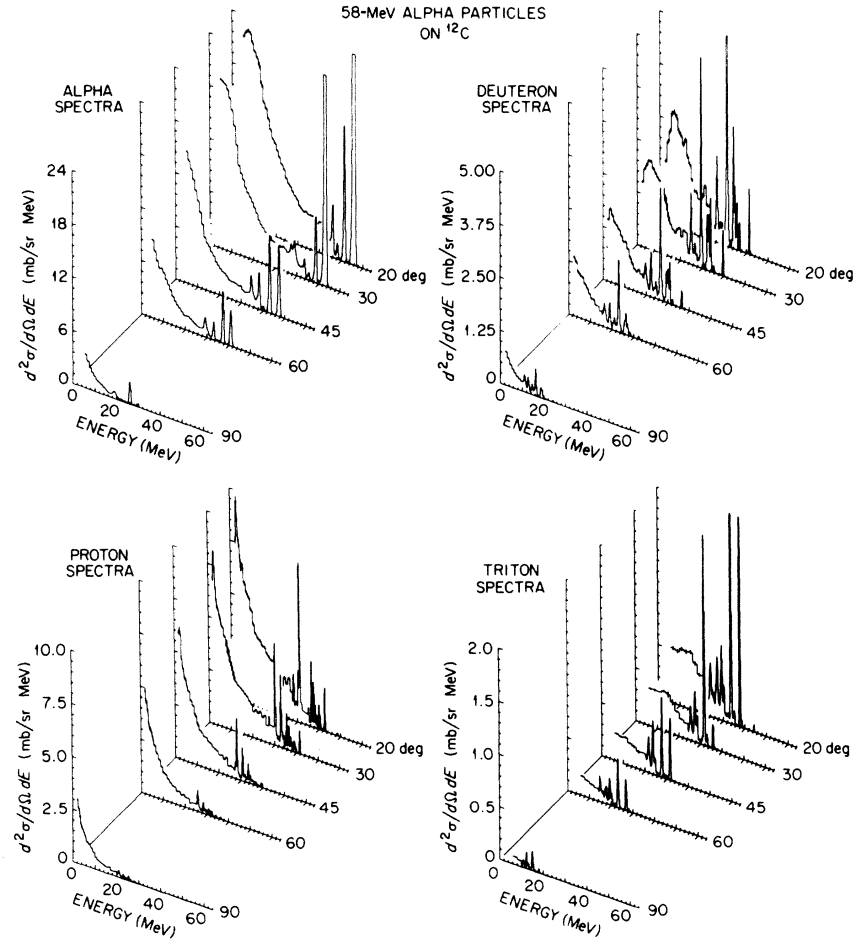

FIG. 2. Proton, deuteron, triton, and α-particle spectra at a few angles from 58-MeV α-particle bombardment of ^{12}C.

discussing other possible structure[16] in the inelastic α-continuum region. We do not interpret our data in these terms because of the uncertainties in the region of possible structure.

Shown in Fig. 6 are the laboratory angle-integrated spectra for the observed charged particles from ^{54}Fe. The integrated laboratory system cross sections, average emitted energies, and low-energy cutoffs are listed in Table I. It is interesting to note that deuteron emission is favored over triton and ^{3}He emission for both ^{54}Fe and ^{12}C (see Fig. 3). Similar results were noted for the production of deuterons by incident protons.[1] If the reaction mechanism were interpreted as a transfer reaction in each case, these results would imply that proton-induced reactions favor transfer of one rather than two nucleons while the opposite is true for incident α particles. Mechanisms involving preequilibrium emission of complex particles are discussed below.

IV. STATISTICAL MODEL CALCULATIONS

A. Model

The preequilibrium model formalism used here is essentially the same as the one used previously[6] in the analysis of complex particle emission in proton-induced reactions. Thus, it is also an extended version of Griffin's basic preequilibrium model.[2] It differs from this previous version in the inclusion of the first order effects of the Pauli exclusion principle and in the use of an empirical prescription for the effective matrix element for the residual two-body interaction.[17] Finally, in integrating the master equations[17] which describe the nuclear equilibration process, it is appropriate in this work to include the loss of strength of the excited composite nucleus due to α, deuteron, triton, and ^{3}He particles, as well as proton and neutron emission. (For Fe at these energies, only proton, neutron, and α particles are required.) All relevant equations can be found in the references quoted above and in a recent report[18] describing the computer program used.

There are several basic assumptions inherent in the model. The most basic assumptions are that a statistical treatment is valid and that, throughout the equilibration process, all states of a given excitation energy with specified numbers of particles and holes are equally likely. The interactions which are responsible for the equilibration are treated using time-dependent perturbation theory and are assumed to be energy-conserving and two-body in nature. The rates for these interactions should also be larger than the particle emission rates, and this point is discussed in some detail in Ref. 19.

Effects which are ignored in the model include shell structure, pairing, angular momentum, and nuclear density effects. The latter effect refers, in particular, to the enhancement of direct transfer reactions in the low nucleon density of the nu-

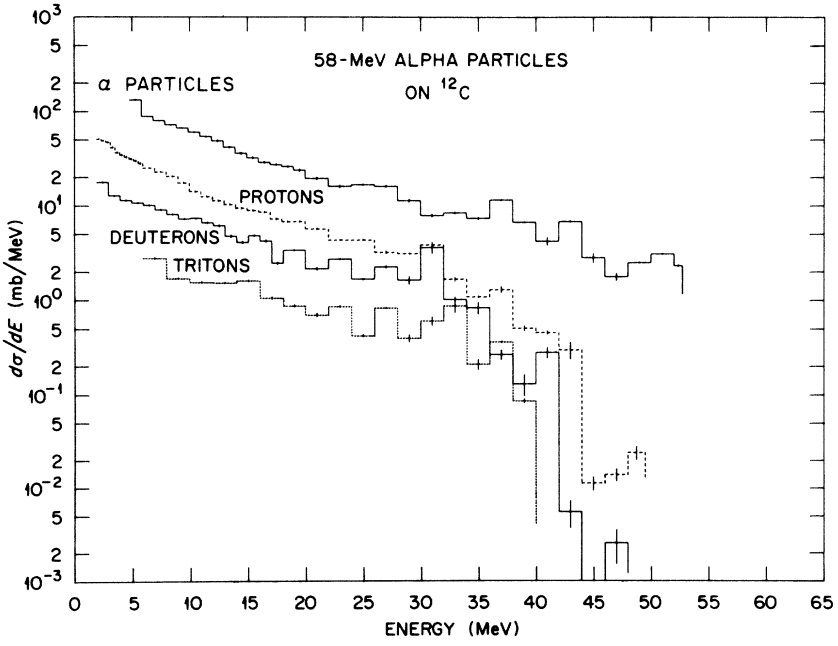

FIG. 3. Angle-integrated (lab system) differential energy spectra for protons, deuterons, tritons, and α-particles from 58-MeV α particles on ^{12}C. Elastic scattering has been excluded from the α spectra.

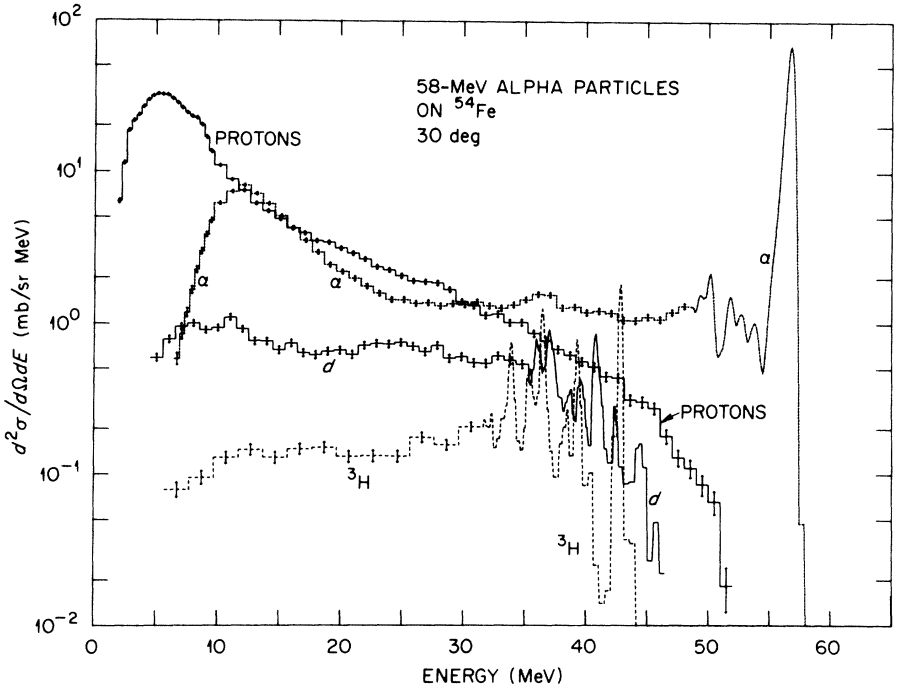

FIG. 4. Proton, deuteron, triton, and α-particle spectra at 30° from ^{54}Fe bombarded by 58-MeV α particles.

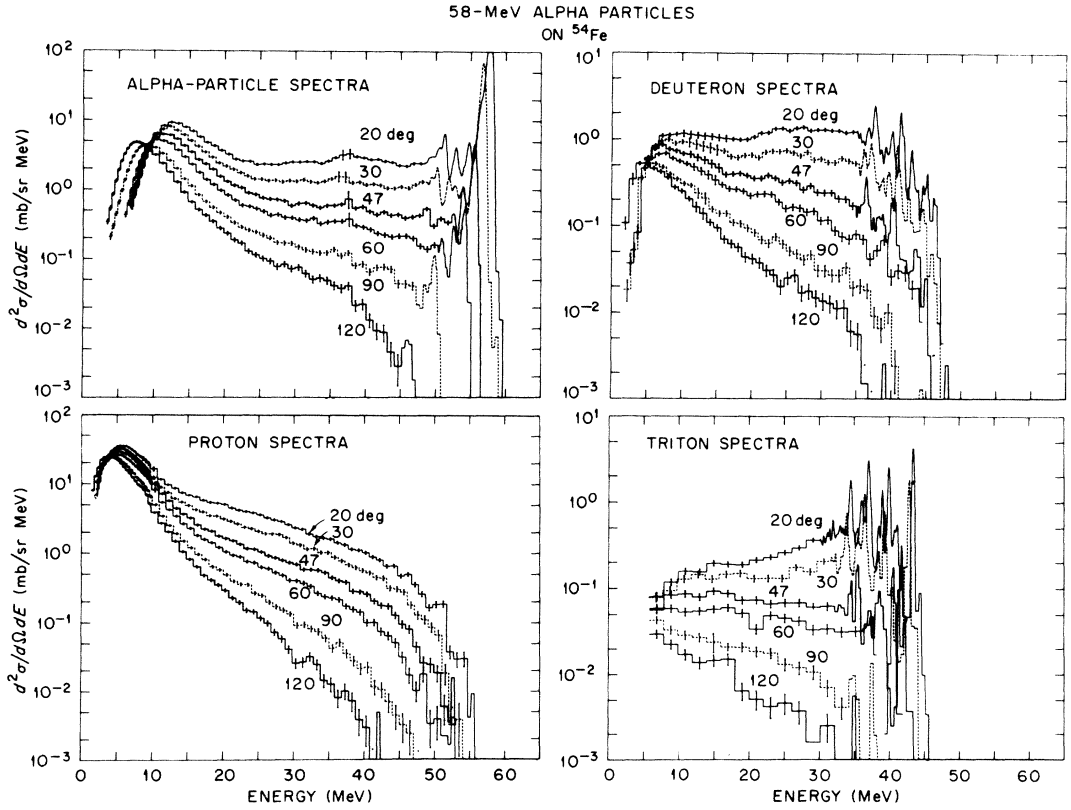

FIG. 5. Proton, deuteron, triton, and α-particle spectra at several angles from 58-MeV α-particle bombardment of ^{54}Fe.

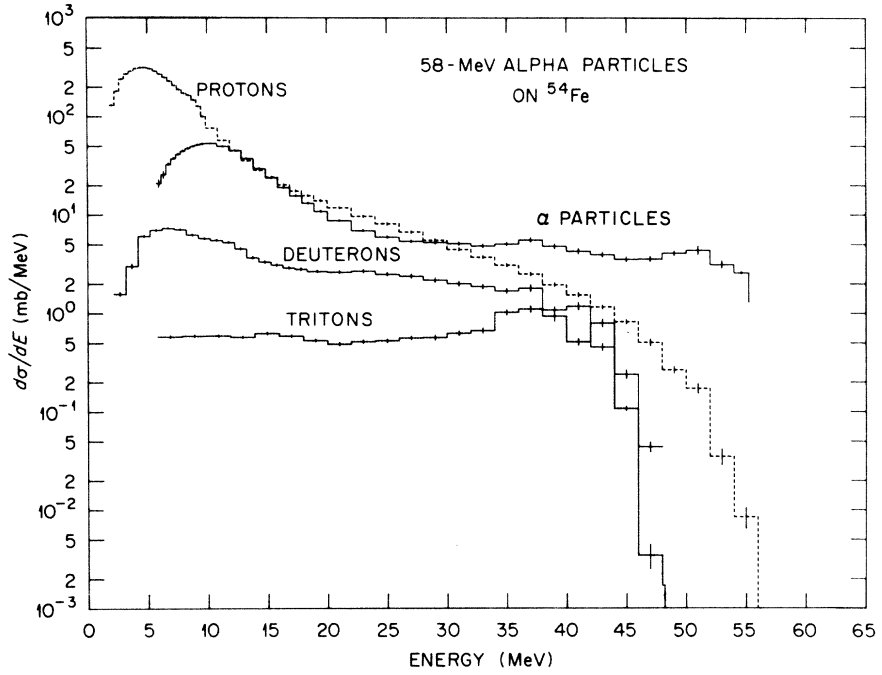

FIG. 6. Angle-integrated (lab system) differential energy spectra for protons, deuterons, tritons, and α particles from 58-MeV α particles on ^{54}Fe. Elastic scattering has been excluded from the α spectrum.

clear surface. Also neglected was emission of more than one preequilibrium particle from a given composite nucleus.

By use of a predetermined empirical prescription for the matrix element for the residual interactions which drive the equilibration process, as well as a fixed single-particle state density and fixed initial exciton configurations, the calculations can predict without free parameters the fraction of the composite nucleus formation cross section which will involve preequilibrium emission of at least one particle. For this study the preequilibrium emission fraction was 80–100%, so that the integrated preequilibrium emission cross section is nearly equal to the composite nucleus formation cross section. All subsequent particle emission was assumed to be equilibrium in nature.

B. Calculations

The preequilibrium part of the calculations was performed using a previously described computer code,[18] modified to include in the master equations the emission of α, deuteron, triton, and ^{3}He particles. All calculations involved numerical integration of the system's master equations. These are[6]

$$\frac{dP(E,p,h,t)}{dt}=\lambda_+(p-1,h-1,E)P(p-1,h-1,t,E)+\lambda_-(p+1,h+1,E)P(p+1,h+1,t,E)-P(p,h,t,E)$$
$$\times\left[\lambda_+(p,h,E)+\lambda_-(p,h,E)+\sum_\beta\int_0^{\epsilon_{\max}}W_\beta(p,h,E,\epsilon)d\epsilon\right], \tag{1}$$

where $P(E,p,h,t)$ is the probability for finding the system in a state with p particles, h holes, and excitation energy E at some time t after the initial target-projectile interaction. The quantities λ_+ and λ_- are, respectively, the rates for particle-hole pair creation and destruction interactions starting from the indicated initial configuration. They have the form,[5]

$$\lambda_+(p,h,E)=\frac{\pi}{\hbar}M^2\frac{g}{(p+h+1)}\left[gE-\frac{(p+1)^2+(h+1)^2}{2}\right]^2,$$

$$\lambda_-(p,h,E)=\frac{\pi}{\hbar}M^2gph(p+h-2),$$

where g is the density of (equally spaced) single-particle states, and M is the average matrix element for the interactions. The quantity

$$W_\beta(p, h, E, \epsilon)$$

is the average rate per unit ϵ for emitting particles of type β and channel energy ϵ from a state with p particles, h holes, and energy E. It is given by

$$W_\beta(p, h, E, \epsilon) = \frac{(2s_\beta + 1)}{\pi^2 \hbar^3} \mu_\beta \sigma_\beta(\epsilon) \epsilon \times d\epsilon \frac{\omega(p - p_\beta, h, U)}{\omega(p, h, E)} R_\beta(p) p_\beta!,$$

where s_β, μ_β, and σ_β are the spin, reduced mass, and inverse cross section for the emitted particle. The quantities $\omega(p, h, E)$ and $\omega(p - p_\beta, h, U)$ are the state densities in the composite and residual nuclei, respectively, and are given by Eq. (2) in Ref. 5. The quantity p_β is the nucleon number of the emitted particle. The factor $R_\beta(p)$, discussed in Ref. 6, gives the probability that p_β nucleons chosen at random from among the p excited ones available will have the right combination of protons and neutrons to make up the outgoing cluster. The term $p_\beta!$ is an empirical adjustment factor found from the analysis of complex particle emission in reactions induced by protons. The exact form of this factor would change for models in which proton-neutron distinguishability was handled more rigorously. Among other things, it covers any "preformation factor" for complex particles inside nuclei. As in equilibrium statistical models, this question is not considered explicitly here. In previous work the sum over β in Eq. (1) was taken to include only neutrons and protons. For this work it was appropriate to include α, deuteron, triton, and ^{3}He particles.

Master equation integration was started assuming a $4p$-$0h$ configuration. Recent analysis[12] of (α, p) data at 54.8 MeV indicates a preference for a four-exciton initial configuration for even-even target nuclides. A four-particle configuration can be visualized as resulting from the "dissolving" of the incident α particles in the nuclear potential. This picture, however, precludes the consideration of such processes as direct α knockout (quasi-free scattering) where the incident α particle acts as a discrete entity. The initial state employed may violate the assumption that all states of the same exciton structure are equally likely at each step in the equilibration process. The density of single-particle states was, as in previous work, taken to be $g = (A/13)$ MeV^{-1} where A is the mass number of the nucleus. The density was calculated separately for the composite and residual nuclei. The square of the average two-body matrix element M^2 was assumed to be given by $M^2 = 1450 \pm 500A^{-3}E^{-1}$ MeV^3 (Ref. 17 value $\times 2$; see Ref. 5).

We have varied the parameters, M^2 and g, and the initial exciton number (n_I) to test the suitability of the generally utilized values to our case. For initial exciton number, we find that our (α, p) and (α, d) results are better described by a 4p-0h configuration than by a 4-1 or 5-0 configuration. This result is in agreement with the work of Ref. 12 which was based only on the (α, p) reaction. It is interesting to note that our measured high-energy ($E \gtrsim 20$ MeV) α inelastic spectra are somewhat better described by $n_I = 5$. Presumably, this is due to the possibility of "first-stage" α-particle emission when $n_I > 4$. However, the calculated inelastic spectra are so poor, compared to the data, that no weight was given to these comparisons in the selection of n_I for our calculations. Variation of M^2 and g gave no evidence that use of other than the usual values, 1450 and $A/13$, respectively, would improve the comparisons. Thus, the values for the model parameters obtained from the behavior of a number of reaction systems[3] were accepted for the comparisons shown here.

The separation energies for the outgoing particles were taken from the mass and Q-value tables of Wapstra and Gove.[20] The inverse cross sections and composite nucleus formation cross sections were approximated by optical model reaction cross sections. For neutrons and protons these were taken from the tabulations of Mani, Melkanoff, and Iori[21] and for α particles on ^{54}Fe the results of Huizenga and Igo[22] were used. For deuterons, tritons, ^{3}He ions, and for α particles on ^{12}C, values were calculated using the code DWUCK[23] and the optical model parameters given in Table II. The absolute normalization of the calculations is determined by the composite nucleus formation cross sections, 410 mb for ^{12}C and 1730 mb for ^{54}Fe.

Since the extended Griffin model does not now include conservation of angular momentum, it is only possible to calculate the angle-integrated spectrum in the center-of-mass system. To allow comparisons, the measured spectra were integrated to give center-of-mass spectra by assuming that each observed particle was the first emitted in the reaction which produced it. Thus, the low-energy portions of the experimental spectra, where multiple emission is important, are distorted in the center-of-mass conversion, particularly for reactions on carbon.

To account for multiple preequilibrium emission, the calculation would have had to keep track of the exciton number and energy of each of the residual nuclei produced by emission of a first preequilibri-

um particle. The equilibration of these residuals would have to be followed to look for emission of a second preequilibrium particle. This has not been done because of the rather tedious nature of the calculations. Instead, the approximation has been made that only one preequilibrium particle is emitted from each nucleus, and subsequent emission occurs only from the equilibrated residual nuclei. At lower initial (composite nucleus) excitation energies, the assumption of no more than one preequilibrium particle per reaction is quite reasonable since the fraction of preequilibrium emission is found to be fairly low, but at 50 or 60 MeV of excitation, the emission of a second preequilibrium particle may have a significant probability (see Ref. 1).

The residual nuclei are assumed to have a distribution of excitation energies determined by the energy spectra of the previously emitted particles. In calculating these distributions, approximate preequilibrium energy spectra were obtained from a closed-form preequilibrium expression given in Eq. (9) of Ref. 6. The Weisskopf-Ewing evaporation formula, with level density parameter $a=(\frac{1}{6}\pi^2)g$, is used for all equilibrium emission calculations in this work. The equilibrium calculations were performed with a computer program which has been previously described[6] and which allows for the emission of up to five particles from the compound nucleus. The net equilibrium spectrum for each particle type is obtained by adding together the spectra for the second and all later members of each possible decay chain.

V. CALCULATIONAL RESULTS AND DISCUSSION

Comparisons between calculated and experimental angle-integrated particle energy spectra are shown in Figs. 7 and 8, while Table III shows a comparison of the energy-integrated cross sections for the different types of emitted particles. The reaction systems are discussed separately.

A. $^{54}Fe + \alpha$ reaction system

The calculated and measured spectral shapes shown in Fig. 7 nearly agree for emitted protons and deuterons, while the experimental triton and α-particle spectra have much more high-energy cross section than is calculated. Changing the $p_\beta!$ normalization factor would not improve the comparisons of Fig. 7.

The agreement in spectral shapes for the protons and deuterons is particularly encouraging because none of the model parameters were varied to achieve it. Systematic empirical values based on other (α, nucleon) spectra were used. Since preequilibrium emission of only one particle per nucleus was considered in the calculations, one might expect to observe the effect of medium-energy second preequilibrium particles in the experimental proton spectrum. There may be some marginal evidence for this in Fig. 7. Such effects should be much smaller in the deuteron and triton spectra because of the fairly large separation energies of these particles.

The underestimation of the high-energy triton emission cross section by the calculations may be the result of a surface enhancement for the single-nucleon direct stripping reaction. A similar behavior may be noted in Fig. 7 of Ref. 6 for the single-nucleon pickup (p, d) reaction also on a ^{54}Fe target. In that case, the low-energy portion of the deuteron spectrum was overestimated in the calculations, but not as seriously as in the present (α, t) results.

TABLE II. Optical model parameters used to compute composite nucleus formation cross sections:

$$U=-V_0(1+e^x)^{-1}-iW_0(1+e^{x'})^{-1}+4a'iW_D\frac{d}{dr}(1+e^{x'})^{-1}+V_C,$$

$$x=\frac{r-r_0A^{1/3}}{a},$$

V_C = Coulomb potential for a uniformly charged sphere of radius,

$R_c=r_cA^{1/3}$.

Particle	Target	V_0 (MeV)	r_0 (fm)	a (fm)	W_0 (MeV)	W_D (MeV)	r_0' (fm)	a' (fm)	r_c (fm)	Ref.
d	^{12}C	77	1.15	0.81	0	22	1.34	0.68	1.15	24
	^{54}Fe	90	1.15	0.81	0	19	1.34	0.68	1.15	24
t	^{12}C	152	1.24	0.678	32	0	1.45	0.841	1.24	25
	^{54}Fe	152	1.24	0.678	26	0	1.45	0.841	1.24	25
^3He	^{12}C	175	1.14	0.723	17	0	1.60	0.81	1.40	26
	^{54}Fe	175	1.14	0.723	17	0	1.60	0.81	1.40	26
^4He	^{12}C	50	1.51	0.576	3.9	0	1.51	0.576	1.51	22

There are several possible explanations for the large deficiency in high-energy α particles in the calculated spectrum. Excitation of strong collective states in the final nucleus accounts for some concentration of strength in the region of high α-particle energies, but this is almost certainly not the whole story. Figure 8 shows the similarity in measured spectral shape for the (p, xp) and $(\alpha, x\alpha)$ reactions on ^{54}Fe and suggests that similar reaction mechanisms may be involved. A mechanism which is thought to be important in the (p, xp) reaction, but which has not been included in the present $(\alpha, x\alpha)$ calculations, is quasifree scattering. In the present calculations, the incident α particle is thought of as "dissolving" in the nuclear potential, but α-nucleon quasifree scattering might make significant contributions to the reaction cross section. Angular momentum effects may also play a role in enhancing the ratio of high-energy α particles to protons in α-particle-induced reactions since α particles can both bring in and carry off more angular momentum than nucleons.

It is apparent from Table III that in spite of the deviations in spectral shapes, the calculations reproduce some of the measured integral cross sections. As was the case for proton-induced reactions, most of the complex particle emission cross section is found to be due to preequilibrium emission.

B. $^{12}C + \alpha$ reaction system

Nuclei between ^{12}C and ^{16}O, the ones involved in the $^{12}C + \alpha$ reaction system, are generally not thought of as good candidates for statistical model analyses. They contain a relatively small number of particles, and their single-particle states are widely spaced in energy. It can be seen from Fig. 2 that much of the $^{12}C + \alpha$ cross section goes into the population of well isolated levels in the residual nuclei. In addition, shell effects in this mass region are quite strong so that the equispacing approximation with $g = (A/13)$ MeV^{-1} should not be expected to be valid.

To first order, the variation in g from one residual nucleus to another should not drastically change the shapes of the calculated spectra[4] but would almost certainly change the relative abundances of the different types of emitted particles. Despite all these objections and partly because of the relatively high bombarding energy used in this work, it was decided to compare the data with preequilibrium model predictions.

The results are shown in Fig. 9. The relative abundances of the different particle types are not well reproduced by the model. However, while the calculation cannot account for the structure observed at the high energies, the calculations do account for the average spectral shapes, yielding better shape agreement for triton and α particles above 20 MeV than was the case for ^{54}Fe.

The numbers in Table III indicate that the calculated intensities obtained using the systematic model parameter values are as much as a factor of six (α particles) in error.

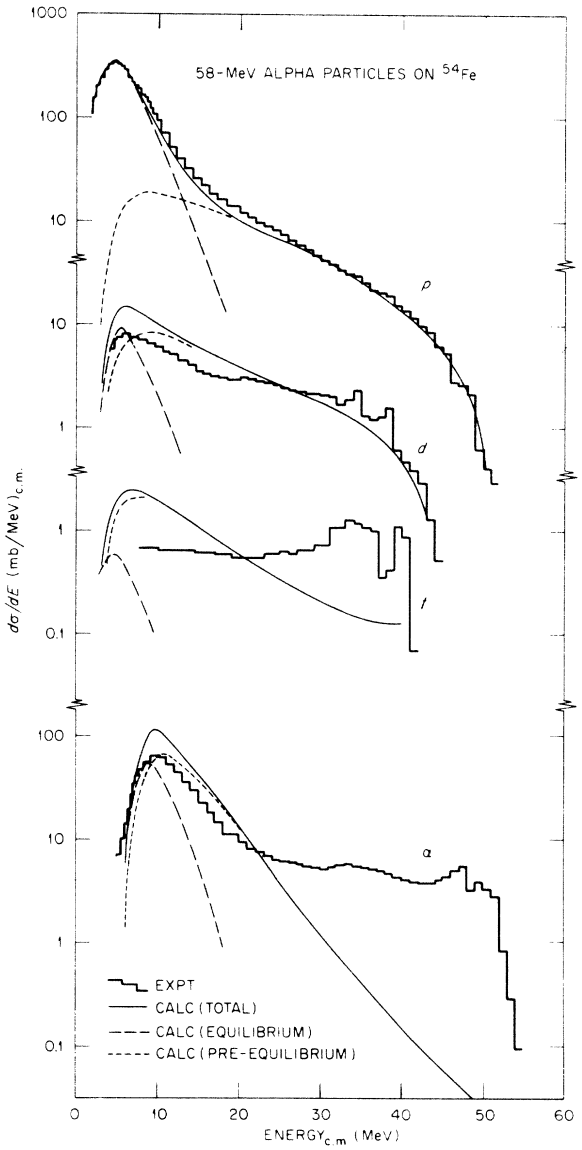

FIG. 7. Comparison of calculated and experimental angle-integrated particle spectra in the c.m. system for 58-MeV α particles incident on ^{54}Fe. The heavy solid histograms show the data; the thin solid curves are the calculated total spectra, while the long- and short-dashed curves show the equilibrium and preequilibrium components of the spectra, respectively. Elastic α scattering is omitted. The low-energy cutoffs on the measured spectra are instrumental in nature.

TABLE III. Experimental and calculated integral emission cross sections in the c.m. system.

Target	Detected particle	Calculation [a] (no cutoff) Pre (mb)	Tot (mb)	Calculation [a] (experimental cutoff) Pre (mb)	Tot (mb)	Experiment [b] Integral cross section (mb)	Cutoff energy (MeV)
^{54}Fe	n	352	1998				
	p	339	2259	339	2259	2255 ± 180	2.1
	d	138	181	136	178	124 ± 10	3.9
	t	28	31	22	22	24 ± 2	7.5
	^{3}He	26	29	19	20	37 ± 14	11.9
	^{4}He [c]	537	807	537	807	660 ± 53	5.2
^{12}C	n	40	230				
	p	53	290	51	211	321 ± 38	3.1
	d	93	176	84	135	121 ± 14	4.6
	t	44	89	28	32	19 ± 2	10.8
	^{3}He	48	82	13	13	13 ± 7	20.4
	^{4}He [c]	117	265	72	77	497 ± 60	12.1

[a] Based on composite nucleus cross sections (σ_R) for ^{12}C and ^{54}Fe of 410 and 1730 mb, respectively.

[b] Errors include uncertainty from all sources for the various targets. No estimate is made for uncertainty due to probable distortion of c.m. spectra due to assumptions made in c.m. conversion (see text).

[c] Excludes elastic scattering.

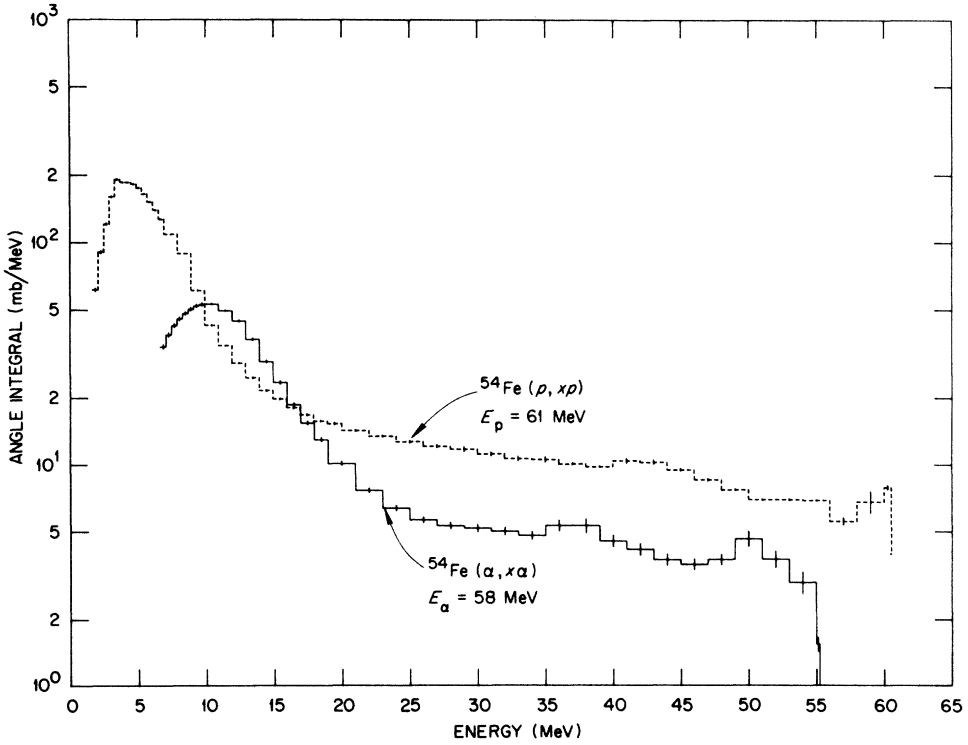

FIG. 8. Comparison of angle-integrated (lab system) (p, xp) and $(\alpha, x\alpha)$ energy spectra. The proton results are for 61-MeV incident protons and were taken from Ref. 1. The distinct shape similarity in the portion of the continuum region not dominated by equilibrium reactions is discussed in Sec. V A of the text.

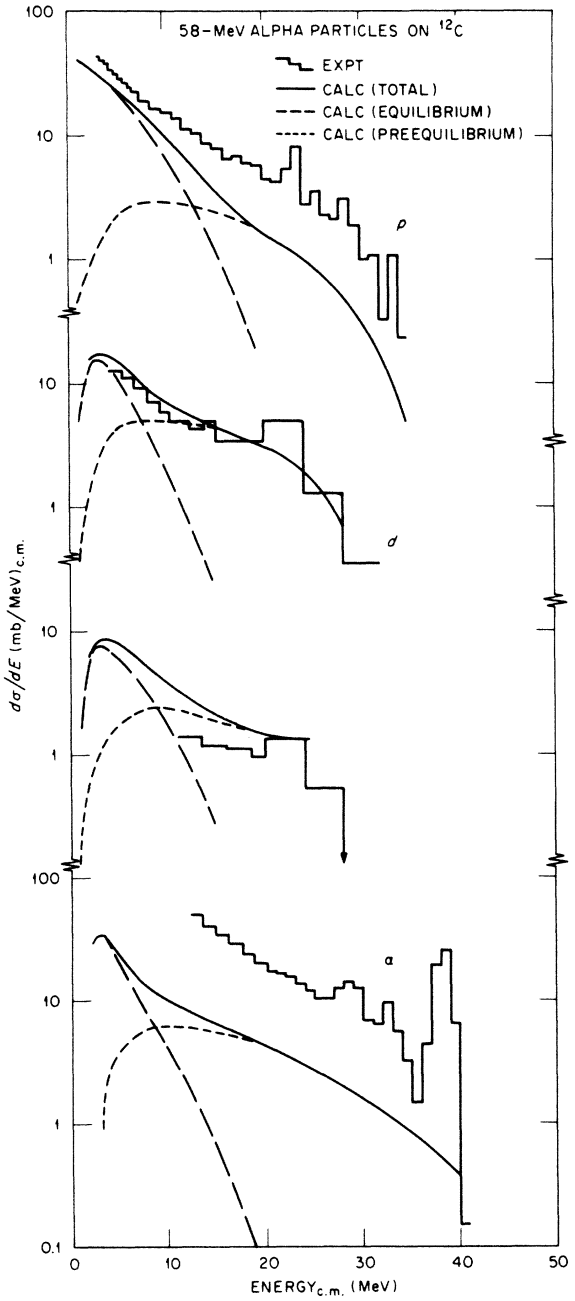

FIG. 9. Comparison of calculated and experimental angle-integrated particle spectra in the c.m. system for 58-MeV α particles incident on ^{12}C. Each curve has the same significance as in Fig. 7. Elastic α scattering is omitted. The strong peak in the α spectrum at $\approx$ 38 MeV is from excitation of the 4.43-MeV level of ^{12}C. The low-energy cutoffs on the measured spectra are instrumental in nature.

VI. CONCLUSIONS

The extended Griffin model seems to have about the same degree of success in accounting for complex particle emission in the $^{54}Fe + \alpha$ reaction system as it did in the analysis of proton-induced reactions (except possibly for deuteron and triton). In both cases high-energy α-particle emission is strongly underestimated, but more so for incident α particles. Spectral shapes are not very accurately reproduced, but the equilibrium calculations clearly account for the measured spectral distribution of the observed particles much better than a pure compound nucleus description. The empirical weighting factor of $p_\beta!$ for the complex particle emission rates seems equally applicable to α-particle-induced reactions and proton-induced reactions.

For the $^{12}C + \alpha$ system, the spectral shapes are surprisingly well reproduced except for details of nuclear structure. However, the abundances of the different particle types were not well accounted for in the calculations.

Again, as in the work of Ref. 6, the significant point is not that the extended Griffin model can reproduce the complex particle spectra perfectly (it cannot), but rather that is can account for a significant fraction of the observed high-energy particles except for α particles and tritons from ^{54}Fe. Complex particle emission is a far more difficult problem to treat in more microscopic preequilibrium models, such as the intranuclear cascade description, and such models have generally not been applied to these reactions. The equilibrium compound nucleus model is, of course, hopelessly inadequate to account for the high-energy complex particles. Thus, it is encouraging that some agreement is obtained between the data and the results of the present calculations.

ACKNOWLEDGMENTS

Many have helped provide the results presented in this paper. We thank T. A. Love, N. W. Hill, W. R. Burrus, H. A. Todd, and C. O. McNew for help in system development; J. D. Drischler and E. Beckham for long hours of help with data analysis; P. M. Aebersold and D. I. Putzulu for imaginative work on data analysis programs; the Oak Ridge Isochronous Cyclotron staff for cyclotron operation; and R. G. Alsmiller and T. A. Gabriel for reviewing the manuscript.

*Research sponsored in part by National Aeronautics and Space Administration Order No. L-12,186 under Union Carbide Corporation's contract with the U. S. Atomic Energy Commission.

†Present address: Service de Physique Nucléaire à Basse Energie, Centre d'Etudes Nucléaire de Saclay,

91 Gif-sur-Yvette, France.
‡Work supported in part by the U.S. Atomic Energy Commission.
§Work supported by the National Science Foundation.
[1]F. E. Bertrand and R.W. Peelle, Phys. Rev. C 8, 1045 (1973).
[2]J. J. Griffin, Phys. Rev. Lett. 17, 478 (1966).
[3]M. Blann, Phys. Rev. Lett. 21, 1357 (1968).
[4]C. K. Cline and M. Blann, Nucl. Phys. A172, 225 (1971).
[5]I. Ribansky, P. Oblozinsky, and E. Betak, Nucl. Phys. A205, 545 (1973). Same expressions except for a factor of two are given in C. K. Cline, Nucl. Phys. A195, 353 (1972).
[6]C. K. Cline, Nucl. Phys. A193, 417 (1972).
[7]F. E. Bertrand, W. R. Burrus, N. W. Hill, T. A. Love, and R.W. Peelle, Nucl. Instrum. Methods 101, 475 (1972).
[8]F. E. Bertrand, R. W. Peelle, T. A. Love, R. J. Fox, N. W. Hill, and H. A. Todd, IEEE Trans. Nucl. Sci. NS-13, 279 (1966).
[9]F. E. Bertrand and R.W. Peelle, ORNL Report No. ORNL-4694, 1971 (unpublished).
[10]L. W. Swenson and C. R. Gruhn, Phys. Rev. 146, 886 (1966).
[11]R. W. West, Phys. Rev. 141, 1033 (1966).
[12]A. Chevarier, N. Chevarier, A. Demeyer, G. Hollinger, P. Pertosa, and Tran Minh Duc, Phys. Rev. C 8, 2155 (1973).
[13]J. Benveniste, G. Merkel, and A. Mitchell, Phys. Rev. C 2, 500 (1970).
[14]M. B. Lewis and F. E. Bertrand, Nucl. Phys. A197, 337 (1972).
[15]L. L. Rutledge and J. C. Hiebert, Phys. Rev. Lett. 32, 551 (1974).
[16]G. Chenevert, N. S. Chant, I. Halpern, C. Glashausser, and D. L. Hendrie, Phys. Rev. Lett. 27, 434 (1971).
[17]C. Kalbach-Cline, Nucl. Phys. A210, 590 (1973).
[18]C. Kalbach-Cline, Univ. of Rochester Report US-NSRL-62 (unpublished).
[19]C. Kalbach-Cline, J. R. Huizenga, and H. K. Vonach, Nucl. Phys. (to be published).
[20]A. H. Wapstra and N. B. Gove, Nucl. Data A9, 265 (1971).
[21]G. S. Mani, M. A. Melkanoff, and I. Iori, Centre d'Etudes Nucléaires de Saclay, Reports Nos. 2379 and 2380, 1963 (unpublished).
[22]J. R. Huizenga and G. Igo, Nucl. Phys. 29, 462 (1962).
[23]Written by P. D. Kunz, Univ. of Colorado (unpublished).
[24]C. M. Perey and F. G. Perey, Phys. Rev. 132, 735 (1963).
[25]J. C. Hafele, E. R. Flynn, and A. G. Blair, Phys. Rev. 155, 1238 (1967).
[26]E. F. Gibson, B. W. Ridley, J. J. Kraushaar, M. E. Rickey, and R. H. Bassel, Phys. Rev. 155, 1194 (1967).